66623

NASA
Technical Memorandum 106360

Army Research Laboratory
Memorandum Report ARL–MR–232

p. 23

Relative Performance Comparison Between Baseline Labyrinth and Dual-Brush Compressor Discharge Seals in a T–700 Engine Test

Robert C. Hendricks
National Aeronautics and Space Administration
Lewis Research Center
Cleveland, Ohio

Thomas A. Griffin and Teresa R. Kline
Vehicle Propulsion Directorate
U.S. Army Research Laboratory
Lewis Research Center
Cleveland, Ohio

Kristine R. Csavina
Sverdrup Technology, Inc.
Lewis Research Center Group
Brook Park, Ohio

Arvind Pancholi and Devendra Sood
General Electric Corporation
Lynn, Massachusetts

Prepared for the
39th International Gas Turbine and Aeroengine Congress and Exposition
sponsored by the American Society of Mechanical Engineers
The Hague, Netherlands, June 13–16, 1994

National Aeronautics and
Space Administration

U.S. ARMY
RESEARCH LABORATORY

RELATIVE PERFORMANCE COMPARISON BETWEEN BASELINE LABYRINTH AND DUAL-BRUSH COMPRESSOR DISCHARGE SEALS IN A T–700 ENGINE TEST

Robert C. Hendricks
National Aeronautics and Space Administration
Lewis Research Center
Cleveland, Ohio 44135

Thomas A. Griffin and Teresa R. Kline
Vehicle Propulsion Directorate
U.S. Army Research Laboratory
Lewis Research Center
Cleveland, Ohio

Kristine R. Csavina
Sverdrup Technology, Inc.
Lewis Research Center Group
Brook Park, Ohio

and

Arvind Pancholi and Devendra Sood
General Electric Corporation
Lynn, Massachusetts

ABSTRACT

In separate series of YT–700 engine tests, direct comparisons were made between the forward-facing labyrinth and dual-brush compressor discharge seals. Compressor speeds to 43 000 rpm, surface speeds to 160 m/s (530 ft/s), pressures to 1 MPa (145 psi), and temperatures to 680 K (765 °F) characterized these tests. The wear estimate for 46 hr of engine operations was less than 0.025 mm (0.001 in.) of the Haynes 25 alloy bristles running against a chromium-carbide-coated rub runner. The pressure drops were higher for the dual-brush seal than for the forward-facing labyrinth seal and leakage was lower—with the labyrinth seal leakage being 2½ times greater—implying better seal characteristics, better secondary airflow distribution, and better engine performance (3 percent at high pressure to 5 percent at lower pressure) for the brush seal. (However, as brush seals wear down (after 500 to 1000 hr of engine operation), their leakage rates will increase.) Modification of the secondary flow path requires that changes in cooling air and engine dynamics be accounted for.

INTRODUCTION

Labyrinth seals are efficient, readily integrated into designs, and generally easy to install into engines but are inherently unstable (Hendricks et al., 1992). However, installing a simple swirl break significantly enhances the stability margin and mitigates this drawback (Childs et al., 1989). Details of theory, experiments, and design methods for labyrinth seals and configurations are provided by Trutnovsky (1977). Forward-facing labyrinth tooth configurations with a variety of rub interfaces (e.g., honeycomb) were studied in detail by Stocker et al. (1977) under a U.S. Air Force contract with codes developed by Morrison and Chi (1985), Demko et al. (1988), and Rhode et al. (1988) and by Rocketdyne (internal Rocketdyne report). Optimization procedures are available from MTI Inc. (private communication from W. Shapiro) and are being implemented into the NASA seals codes program.

Brush seal systems are efficient, stable, contact seals that are usually interchangeable with labyrinth shaft seals but require a smooth rub runner interface and an interference fit upon installation. The major unknowns and needed research are tribological (e.g., life or interface friction and wear) because of the following performance demands: pressure drops over 2.1 MPa (300 psi), temperatures to over 1090 K (1500 °F), and surface speeds to 460 m/s (1500 ft/s). Current research supported by the Navy (private communication from W. Voorhees), the U.S. Army (private communication from R. Bill and G. Bobula), and the U.S. Air Force's Wright Patterson Air Force Base is addressing these issues and shows promise in meeting these demands.

In this paper we compare the relative pressure drop differences between the baseline labyrinth and dual-brush compressor discharge seals at compressor discharge pressures to 1 MPa (145 psi) and temperatures to 680 K (765 °F) with operating speeds to 43 000 rpm.

ENGINE FLOW PATH

The power stream airflow through the compressor and the secondary airflow leakage past the compressor discharge seal (CDP) are illustrated in Fig. 1(a), and the CDP viscous-tube flowmeter is shown in Fig. 1(b). The compressor discharge seal package and associated drain tube are located immediately downstream of the impeller and labeled CDS. The drain tube was opened after a series of runs and swabbed for debris.

COMPRESSOR DISCHARGE SEAL

Labyrinth Seal System

The labyrinth CDP seal package and airflow path are shown in Fig. 2(a). The nominal 71-mm (2.8-in.) diameter forward-facing labyrinth seal system is illustrated in Fig. 2(b). The labyrinth teeth rub into a felt-metal type of interface, forming the seal system. Note that the teeth are not all forward facing and are used in different ways to satisfy different engine operating requirements. A simulated exploded view of the seal system is given in Fig. 3 and clearly illustrates the forward-facing teeth of the rotor. However, the housing shown in the figure is for the brush seal.

Brush Seal System

The dual brush was selected over a single brush for reliability of a critical engine component, distribution of the pressure drop per brush, and mitigation of wear. The dual-brush CDP seal package and airflow path are shown schematically in Fig. 4(a) and illustrated in Fig. 4(b). The dual brush, nominally 71 mm (2.8 in.) in diameter, runs against a 0.178- to 0.254-mm (0.007- to 0.010-in.) thick, smooth (8 rms) chromium-carbide-coated rub runner interface as shown schematically in Fig. 4(c). (See also Figs. 11(b) and (c) between wear scars.) The basic seal system was envisioned by General Electric and manufactured by Cross Mfg. Ltd. (Flower, 1990). It has 0.071-mm (0.0028-in.) diameter, Haynes 25 bristles angled 43° to 50° to the interface with approximately 98 to 99 per millimeter of circumference (2500 per inch of circumference) and a nominal interference fit of 0.127 mm (0.005 in.) at installation. Brush seal design conditions include surface speed of 168 m/s (550 ft/s), temperature of 740 K (870 °F), pressure drop of 0.6 MPa (84 psi), and bristle deflection of 0.64 mm (0.025 in.). Figure 5 gives a post-test exploded view of the brush seal system with associated instrumentation lines (cut after testing). Figure 6 provides a side-by-side comparison of the forward-facing labyrinth seal (right) and the chromium-carbide-coated rub runner replacement (left); these represent the rotating interface. This design could be enhanced by using an upstream "washer" to mitigate foreign object damage and by optimizing the backing washer thickness and profile to pressure loading to mitigate hysteresis.

APPARATUS AND INSTRUMENTATION

Pretest and post-test photographs of the dual brush and its installation in the seal system are shown in Figs. 4, 5, and 7. Figure 4(b) depicts the dual brush prior to and Fig. 5 after testing. Figure 7(a) shows the upstream view of the instrumented housing; four thermocouples are attached to the side plates with upstream and downstream pressure taps. Figure 7(b) shows a direct view from the downstream side, and Fig. 7(c) is an isometric view showing the "shiny" nature of the bristle interface. Many seal dimensions and coating and installation details are proprietary.

ENGINE SEAL INSTALLATION AND OPERATIONS

The YT–700 compressor section was first assembled with the labyrinth seal and run as a baseline for comparison. After a test series was completed, the engine was shipped to the Corpus Christi overhaul facility. The compressor discharge seal labyrinth system was removed and the brush package (Fig. 8(a)) inserted into the housing (Fig. 8(b)). The brush seal system was installed without special waxes, which can lead to bristle distortions and irregular bristle voidage. (These waxes hold the bristles off the rotor during installation and readily "burn out" at a low temperature.) The installation was blind; a pencil run about the circumference spread the bristles uniformly, and the shaft rotated as the package was inserted vertically into the engine.

Operations consisted of the standard break-in procedures with data taken primarily under steady conditions. The engine was operated a total of 46 hr, including break-in, from ground to power-turbine-inlet-temperature-limited full power. Compressor speeds were to 43 000 rpm with seal housing temperatures to 680 K (765 °F). Local conditions at various compressor discharge pressures are given in Tables I and II. The compressor discharge seal leakage was vented through the drain tube (Fig. 1) and metered using the tube as a viscous flowmeter. The debris collected in the drain tube was a "lubricant powder," but the spectra indicated several contaminant metals from elsewhere in the engine. Rotor roughness, brush construction, and upstream debris generation play a major role in determining the spectrum. Although neither radial nor axial rotor positions were monitored, such position sensors should be an integral part of the engine dynamics.

RESULTS

Post-test measurements of the brush and inspection of the bristles revealed a smooth bristle interface with some characteristic shear wear (Fig. 9) but little other visible damage. From an unrecorded visual inspection at 64X prior to test, the bristle tips were sharp, clean, elliptical surfaces. The brush wear patterns (Figs. 10 and 11) were attributed to the engine dynamics although no dynamic tracking instrumentation was available. The patterns are interesting in that they are on the average 15° from the antirotation pin. (The clocking point may be associated with a compressor bearing position or loading point.) The patterns for the upstream seal differed from those for the downstream seal (see also Fig. 4), indicating a differential in pressure drop across each of the seals. It is anticipated that about 40 percent of the total pressure drop across the dual brush occurred across the first brush and 60 percent across the second brush (Flower, 1990, and private communication from R. Flower of Cross Mfg. Ltd.). Such loading resulted in stiffer bristles in the second brush and implies a greater bristle wear. Preload and operational loads are important design life parameters (private communication from Ellen Mayhew of Wright Patterson Air Force Base), but data to quantize these parameters are not available.

Another variation in the wear pattern is attributed to the rotor machining or coating variations (Fig. 11(a)). The rotor showed a small eccentricity and was investigated for metallic transfer, but no significant transfer was found. The chromium carbide interface was worn smoother by the rubbing brush bristle interface, implying some form of wear or material smearing without significant transfer of the chromium carbide (CrC is usually a plasma-sprayed mixture of Cr_3C_2 and Cr_7C_3 ground and polished to form the rub-runner surface). The CrC-coated rub runner exhibited slight wear scars but no spallation or coating degradation otherwise, as illustrated in Fig. 11(b); however, eccentric operations, startup, or a hard rub caused a deeper scar over about 120° of the rotor as shown in Fig. 11(c). These wear bands are readily visible in Fig. 6, where the upper band is associated with the upstream (high-pressure side) brush; see also Figs. 5 and 8.

During the test series the drain pipe (Fig. 1) was swabbed for debris. When these samples were in turn investigated with a scanning electron microscope (SEM), nickel, chromium, and tungsten lines were observed along with other unexplainable peaks of salts (e.g., Fig. 12). The nickel, chromium, and tungsten lines characterize bristle materials and some possible coating wear. The debris was fine and difficult to locate and isolate within the tube. Other metal sources and rubbing surfaces could have also produced such debris, but we attributed it to bristle wear.

The upstream wear surface of the rub runner is characterized by Fig. 13(a) and the downstream wear surface by Fig. 13(b). The CrC coating is characterized by light and gray areas, and the energy spectrum shows the light areas to be an NiCr composition and the gray areas to be predominantly Cr. The light and gray areas of the matrix or unrubbed material between the bands is illustrated in Figs. 13(c) and (d). Similarly, for the upstream wear band in Figs. 13(e) and (f) and for the downstream wear band in Figs. 13(g) and (h). There appears to be no material transfer from the bristles to the rotor and only minor scarring and polishing.

The result of interest here is that the initial design interference was 0.127 mm (0.005 in.) and the post-test estimate of interference was 0.101 mm (0.004 in.), or perhaps a maximum wear of 0.025 mm (0.001 in.).

Representative seal leakage variations as a function of compressor discharge pressure are given as Fig. 14, with calculation parameters in Table I. (See Fig. 1(b) for the location of the flowmeter.) Readings 42 to 111 are labyrinth or baseline seal data; readings 331 to 342 are dual-brush seal data. On the average the labyrinth seal leakage is 2.5 times more than the dual-brush seal leakage and strongly depends on pressure relative to the dual brush. Increasing pressure tends to pack the dual-brush seal; leakage flow decreases to approximately 0.83 MPa (120 psi) and then increases. (It also stiffens the bristles and increases wear.) The pressure drops for each comparable compressor discharge pressure setting were higher for the brush seal system than for the labyrinth seal system (Tables I to III). For the same engine operating conditions the dual-brush system leaked less than the baseline forward-facing labyrinth seal system. Also implied is enhanced engine efficiency. However, a decrease in experimental testbed engine specific fuel consumption (3 percent at compressor discharge pressures of 1 MPa (145 psi) to 5 percent at 0.62 MPa (90 psi)) was found (Fig. 15, Table IV). Variation of experimental testbed specific fuel consumption with horsepower is given in Fig. 16. To within the error estimates the performance increase is assumed to result from less leakage and enhanced distribution of secondary airflow through the engine.

It is important to recognize that more efficient seals cannot simply be installed without computing and accounting for the secondary airflows necessary for the cooling and engine dynamics associated with the seal leakage modifications.

SUMMARY

In a series of YT-700 engine tests, direct comparisons were made between a forward-facing labyrinth seal configuration and a dual-brush compressor discharge seal. The nominal seal diameter was 71 mm (2.8 in.). The test conditions included compressor discharge pressures to 1 MPa (145 psi), temperatures to 680 K (765 °F), operating speeds to 43 000 rpm, and surface speeds to 160 m/s (530 ft/s) with the working fluid being nominally dry ambient air. The bristle wear was estimated to be less than 0.025 mm (0.001 in.) in 46 hr of engine operations.

The average labyrinth seal leakage was 2½ times greater than the dual-brush seal leakage and strongly dependent on pressure; the dual-brush leakage was weakly pressure dependent and brush packing effects were noted. The experimental testbed specific fuel consumption was less for the dual brush than for the labyrinth seal—3 percent less at high compressor discharge pressure and 5 percent less at lower pressure. Decreased seal leakage and better distribution of secondary airflow are assumed to account for the performance increases. (However, as brush seals wear down (after 500 to 1000 hr of engine operation), their leakage rates will increase.)

More efficient seals cannot simply be installed into an engine without computing and accounting for the secondary airflows necessary for the cooling and engine dynamics associated with the seal leakage modifications.

ACKNOWLEDGMENTS

The authors wish to thank Philip Abel, Robert Bill, George Bobula, Dennis Bors, Anthony Bright, Chris Conrad, Edward Chisolm, Dan Erbacher, Dave Evanoff, Joe Flowers, Stephen Grozner, Tim Hawk, Paul Lemermeier, Kazhuhisa Miyoshi, Karl Owen, Edith Parrott, Jeffry Paulin, Barry Piendl, Joe Shivak, Don Striebing, Queito Thomas, and the Corpus Christi Army Depot T-700 Engine Assembly Area.

REFERENCES

Childs, D.W., Ramsey, C.J., and Pelletti, J.M., 1989, "Rotordynamic-Coefficient Test Results for the SSME HPOTP Turbine Interstage Seal for the Current and Improved Swirl

Brake," NASA Lewis Grant NAG3–181, Turbomachine Laboratories Report 338–TL–3–89, Texas A&M University, College Station, TX 77843.

Demko, J.A., Morrison, G.L., and Rhode, D.L., 1988, "The Prediction and Measurement of Incompressible Flow in a Labyrinth Seal," AIAA Paper No. 88–0190.

Flower R., 1990, "Brush Seal Development Systems," AIAA Paper 90–2143.

Hendricks, R.C., Carlile, J.A., and Liang, A.D., 1992, "Some Sealing Concepts—A Review. Part A–Industrial, Proposed, and Dynamic; Part B–Brush Seal Systems," Presented at the ISROMAC–4, The Fourth International Symposium of Transport Phenomena and Dynamics of Rotating Machinery, Honolulu, HI, U.S.A., Apr. 5–8.

Morrison, G.L., and Chi, D., 1985, "Incompressible Flow in Stepped Labyrinth Seals," ASME Paper No. 85–FE–4.

Rhode, D.L., Ko, S.H., and Morrison, G.L., 1988, "Numerical and Experimental Evaluation of a New Low Leakage Labyrinth Seal," AIAA/ASME/SAE/ASEE 24th Joint Propulsion Conference, July 11–13, 1988, Boston, MA, Paper No. 88–2884.

Stocker, H.L., Cox, D.M., and Holle, G.F., 1977, "Aerodynamic Performance of Conventional and Advanced Design Labyrinth Seals With Solid-Smooth, Abradable, and Honeycomb Lands," NASA CR–135307.

Trutnovsky, K., 1977, "Contactless Seals. Foundations and Applications of Flows Through Slots and Labyrinths," NASA TT F 17352.

TABLE I.—PARAMETERS FOR CALCULATING SEAL LEAKAGE VARIATIONS

[CDP viscous-tube flowmeter diameter, 0.625 in.]

Reading	Compressor discharge pressure, psia	Temperature, °F	Total pressure, psi	Static pressure, psi	Pressure ratio	Velocity, ft/s	Volumetric flow rate, ft^3/s	Standard volumetric flow rate, ft^3/s	Density, lb/ft^3	Weight flow rate, lb/s
42	70	498.37	16.31	16.08	0.985898	178.3516	0.379983	0.225091	0.045303	0.010197
49	90	578.11	17.39	17.05	.980449	208.8661	.444995	.258028	.044345	.011442
56	145	764.85	22.15	21.52	.971558	256.2389	.545924	.338611	.047436	.016062
63	90	581.32	17.48	17.13	.979977	211.4514	.450503	.261638	.044416	.011621
71	70	504.08	16.32	16.08	.985294	181.7921	.387313	.228074	.045035	.010271
96	120	687.96	19.73	19.2	.973137	248.0307	.528437	.312021	.045157	.01409
103	143	764.84	21.94	21.33	.972197	252.9277	.53887	.331287	.047017	.015576
111	120	689.97	19.78	19.25	.973205	247.6759	.527681	.31184	.045196	.014094
331	80	439.87	15.96	16.01	1.003133	73.59044	.156787	.098485	.04804	.004731
332	90	485.28	16.55	16.61	1.003625	70.39595	.149981	.093044	.047445	.004414
333	120	586.86	18.3	18.41	1.006011	54.75435	.116656	.072427	.047482	.003439
334	145	656.26	20.29	20.37	1.003943	68.33075	.145581	.093789	.04927	.004621
335	155	691.24	21.24	21.34	1.004708	63.33183	.13493	.088299	.050047	.004419
336	162	709.28	21.95	22.06	1.005011	61.34261	.130692	.087046	.050938	.004434
337	162	711.44	22.02	22.1	1.003633	70.34602	.149874	.099819	.050936	.005084
338	155	698.44	21.44	21.51	1.003265	72.73489	.154964	.101581	.050132	.005093
339	145	667.55	20.49	20.56	1.003416	71.7534	.152873	.098409	.049231	.004845
340	120	596.94	18.55	18.63	1.004313	65.91849	.140441	.087395	.047591	.004159
341	90	509.82	16.72	16.78	1.003589	70.63543	.150491	.091929	.046717	.004295
342	80	467.61	16.14	16.21	1.004337	65.75922	.140102	.086439	.047185	.004079

TABLE II.—T-700 COMPRESSOR DISCHARGE SEAL AND ENGINE TEST PARAMETERS

(a) On way up

Configuration	Compressor speed, rpm	Turbine speed, rpm	Compressor discharge pressure, psia	CDLPCE[a] temperature, °F	Impeller aft cavity pressure, psia	CDLPCE pressure, psia	Pressure difference, psia
Baseline	29 600	10 500	50	348	37.5	16.2	21.3
Brush				321	39.5	15.4	24.1
Difference							2.8
Baseline	35 500	14 000	70	498	46.7	17.0	29.7
Brush[b]			79	458	53.1	16.3	36.8
Difference							7.1
Baseline	38 300	17 400	90	578	57.5	18.4	39.1
Brush				502	59.2	16.8	42.4
Difference							3.3
Baseline	41 300	20 000	120	688	74.2	21.2	53.0
Brush	40 400	20 000		599	76.0	18.7	57.3
Difference							4.3
Baseline	43 190	19 000	145	765	87.6	23.9	63.7
Brush	42 340	20 000		673	89.9	20.8	69.1
Difference							5.4
Baseline and brush	43 090	19 700	155	710	95.6	21.8	73.8

(b) On way down

Configuration	Compressor speed, rpm	Turbine speed, rpm	Compressor discharge pressure, psia	CDLPCE[a] temperature, °F	Impeller aft cavity pressure, psia	CDLPCE pressure, psia	Pressure difference, psia
Baseline and brush	42 500	20 000	145	683	89.9	20.9	69.0
Baseline	41 400	20 000	120	690	74.1	21.2	52.9
Brush				605	76.4	18.9	57.5
Difference							4.6
Baseline	38 400	17 400	90	581	57.7	18.5	39.2
Brush	37 800	18 100		516	59.1	16.9	42.2
Difference							3.0
Baseline	35 600	14 000	70	—	46.8	16.9	29.9
Brush	34 800	14 600		473	48.2	16.0	32.2
Difference							2.3
Baseline	29 700	10 500	50	378	37.6	16.1	21.5
Brush	31 700	10 500	59	379	42.9	15.8	27.1
Difference							5.6

[a]CDLPCE denotes compressor discharge low-pressure-cavity exhaust.
[b]rpm overshot and then backed down to "run through" the compressor critical speed. (Note: this is not the case on the way down.)

TABLE III.—RELATIVE PRESSURE DROPS FOR BASELINE COMPRESSOR DISCHARGE LABYRINTH AND BRUSH SEAL SYSTEMS

(a) On way up

Compressor discharge pressure, psia	Pressure difference, $\Delta P_{brush} - \Delta P_{baseline}$, psi
50	2.8
[a]70, [b]79	7.1
90	3.3
120	4.3
145	5.4

(b) On way down

Compressor discharge pressure, psia	Pressure difference, $\Delta P_{brush} - \Delta P_{baseline}$, psi
120	4.6
90	3.0
70	2.3
[a]50, [b]59	5.6

[a]Baseline.
[b]Brush.

TABLE IV.—DECREASE IN SPECIFIC FUEL CONSUMPTION WITH INCREASE IN COMPRESSOR DISCHARGE PRESSURE FOR DUAL-BRUSH SEAL

Reading	Compressor discharge pressure, psia	Experimental testbed engine specific fuel consumption	Experimental testbed engine horsepower
42	70	1.38	139
49	90	.95	140.9
56	145	.59	185.6
63	90	.96	193.9
71	70	1.36	265.8
96	120	.67	265.8
103	143	.59	270.4
111	120	.68	278.1
331	80	1.12	552.8
332	90	.92	545.4
333	120	.67	538
334	145	.57	552.5
335	155	.55	828.9
336	162	.54	839.6
337	162	.53	822.8
338	155	.54	828.8
339	145	.57	953.6
340	120	.66	990.1
341	90	.9	1038.3
342	80	1.11	1060.9

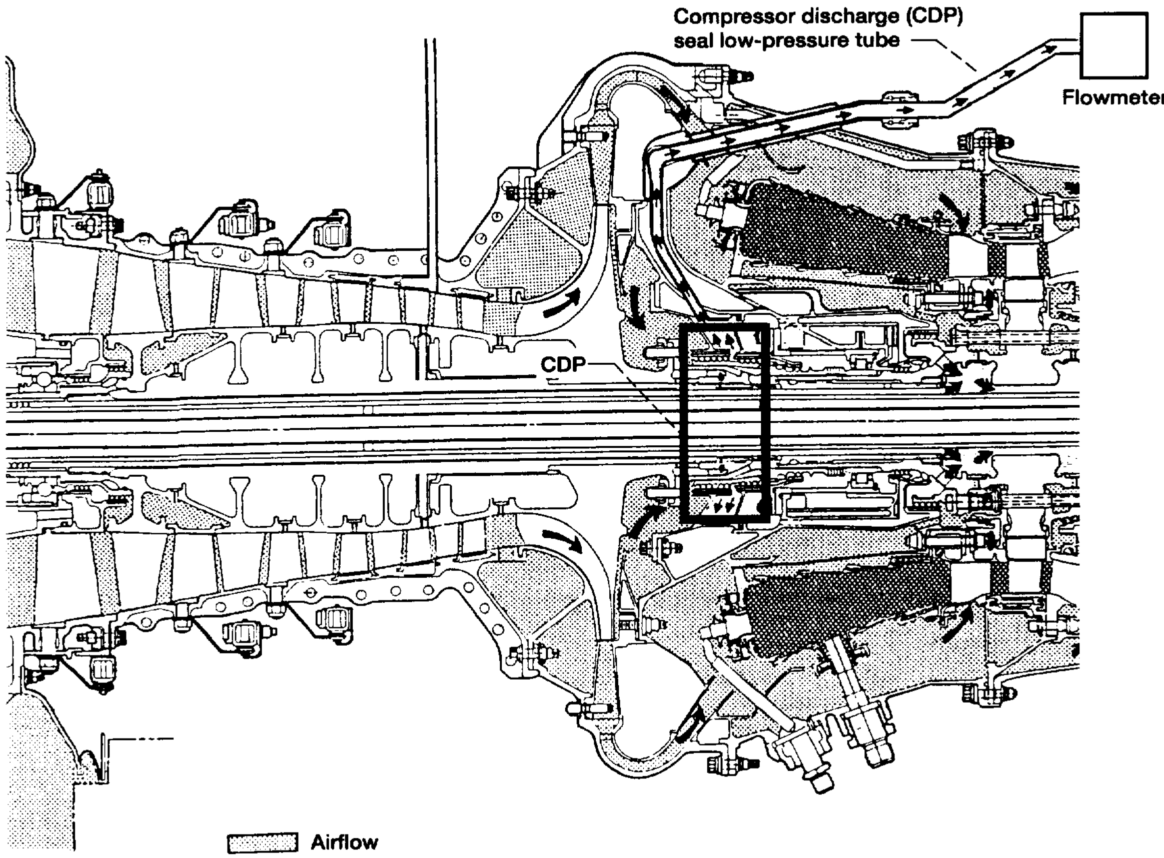

(a) Airflow schematic.

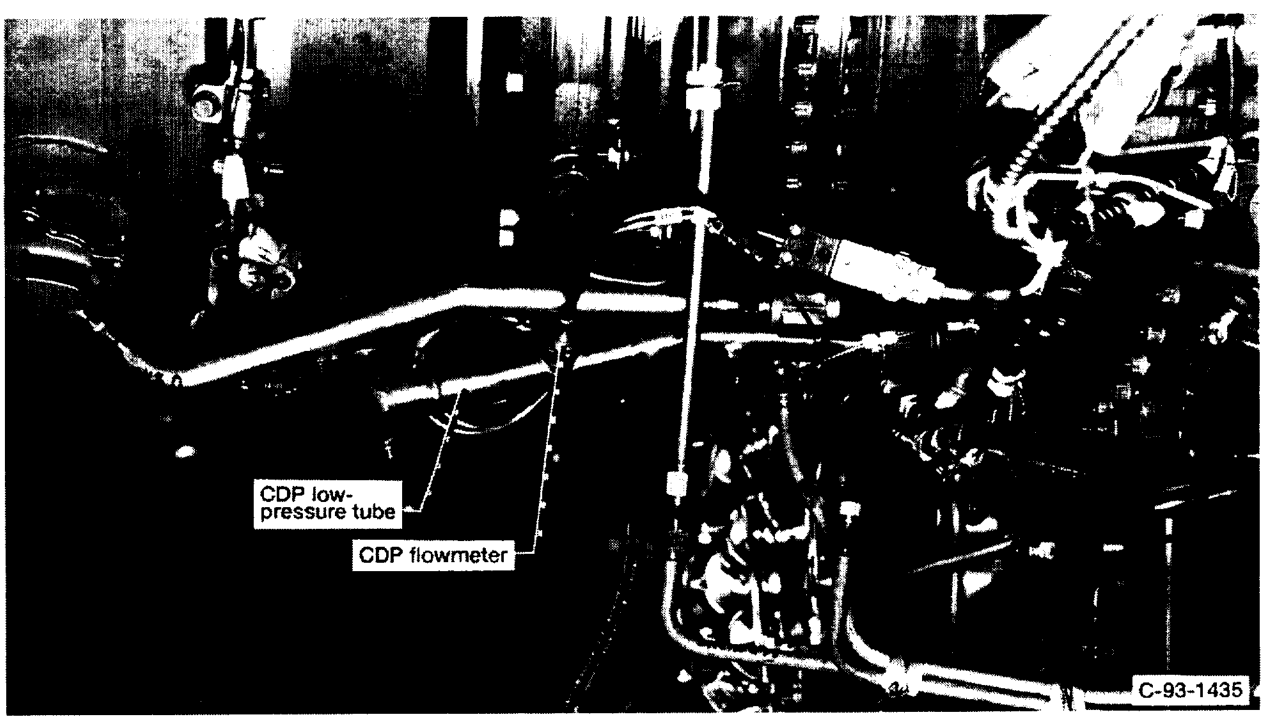

(b) Location of CDP flowmeter.

Figure 1.—Schematic of engine airflow and location of flowmeter.

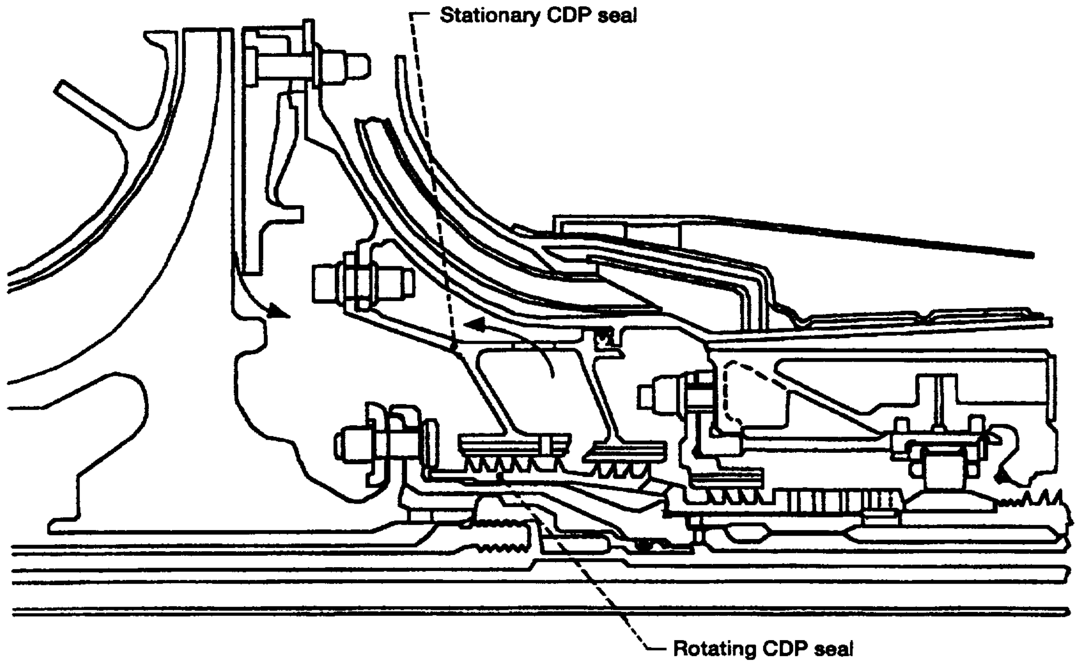

(a) Labyrinth seal package and airflow.

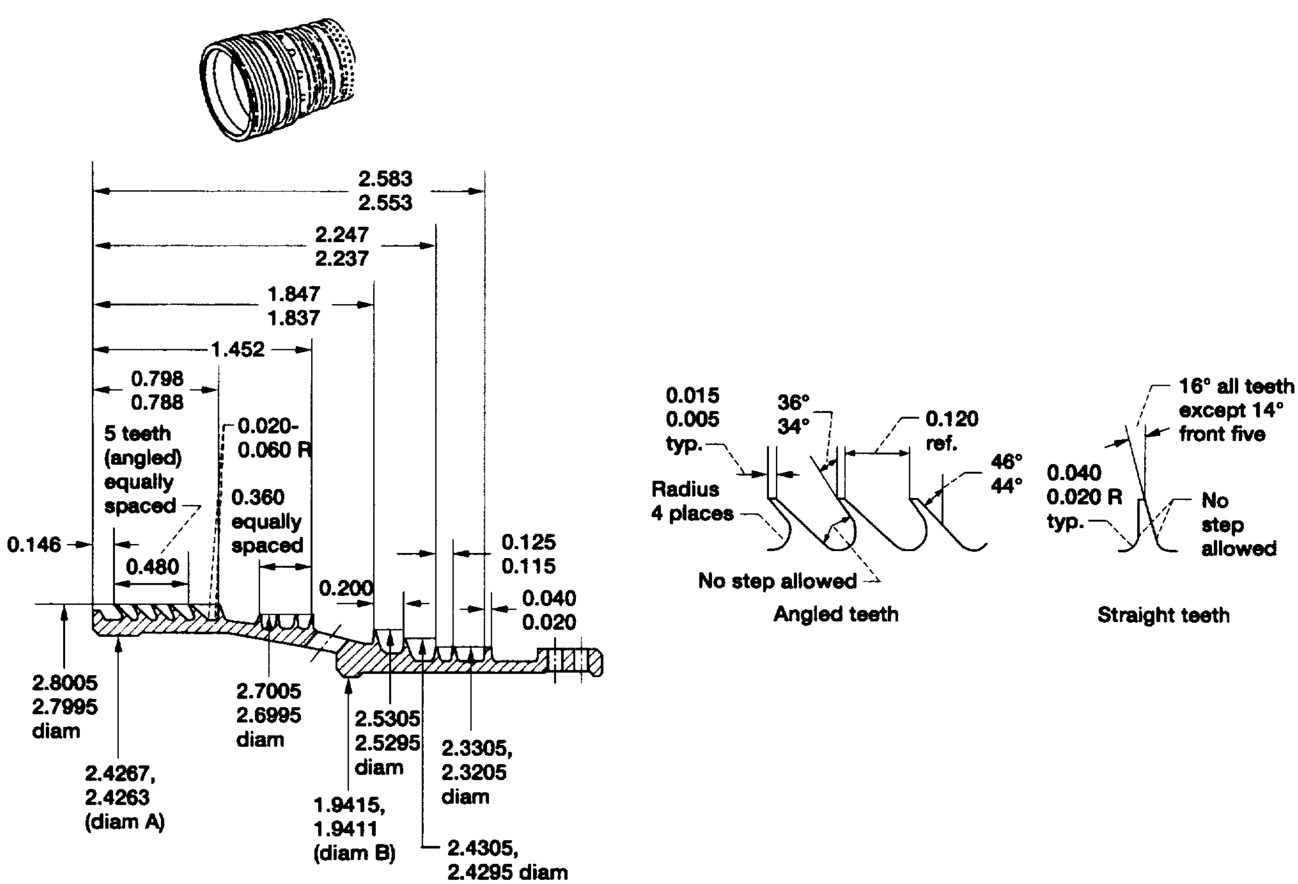

(b) Schematic of labyrinth compressor discharge seal. (Seal teeth and axis established by diameters A and B to be concentric within 0.003 full indicator reading. No steps allowed on tooth face or at fillet radius. All dimensions are in inches.)

Figure 2.—Labyrinth compressor discharge seal system.

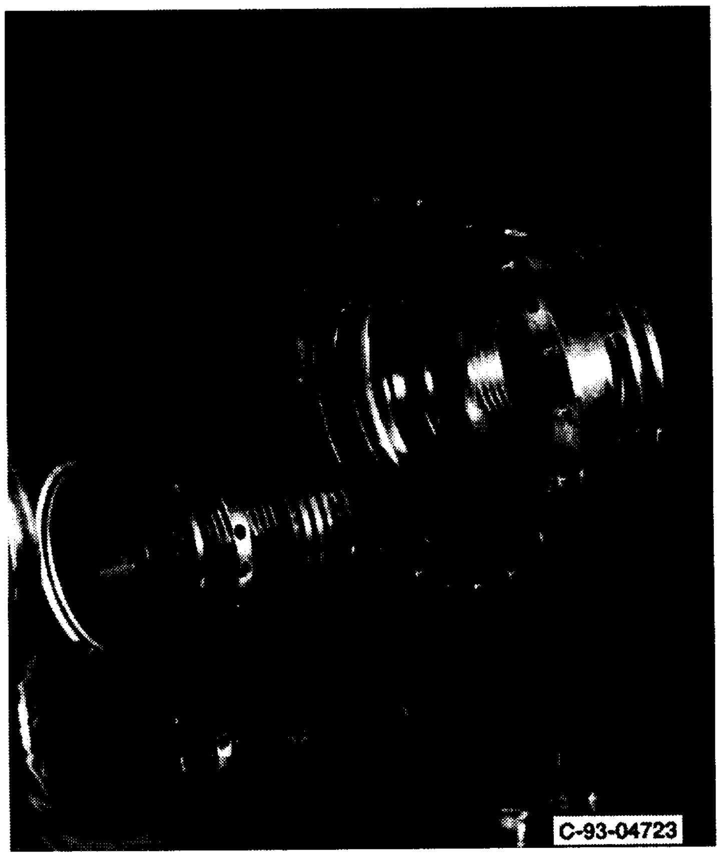

Figure 3.—Simulated exploded view of labyrinth compressor discharge seal system.

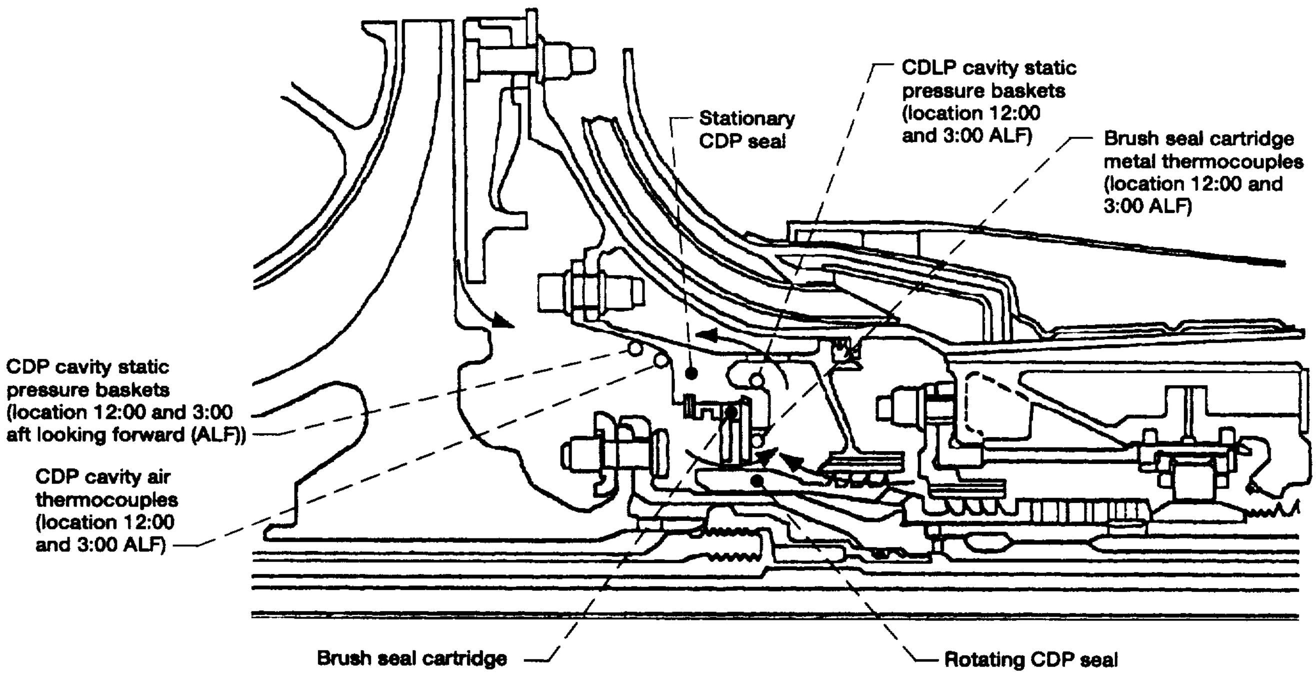

(a) Brush seal package and airflow.

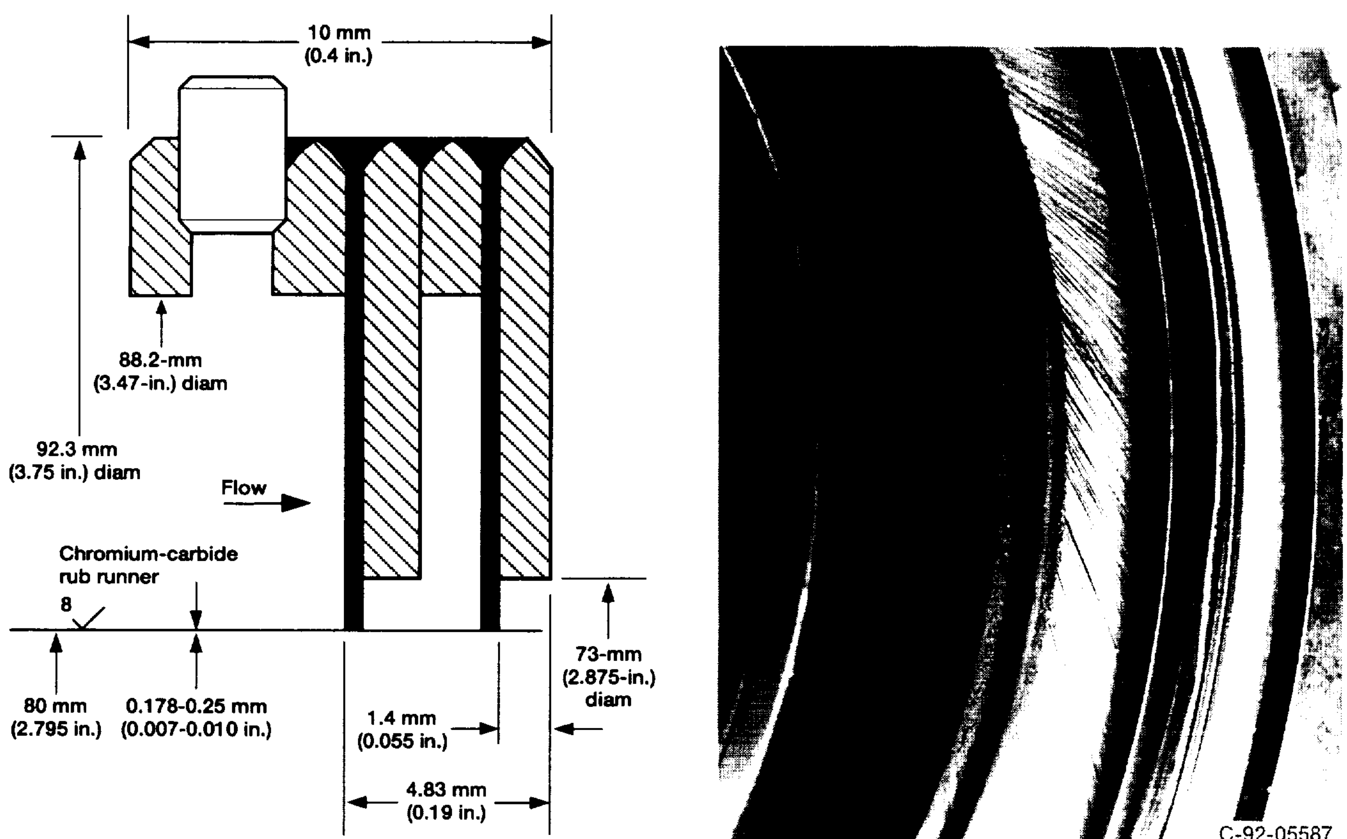

(b) Illustration of dual-brush compressor discharge seal system.

Figure 4.—Dual-brush compressor discharge seal system and schematic of airflow.

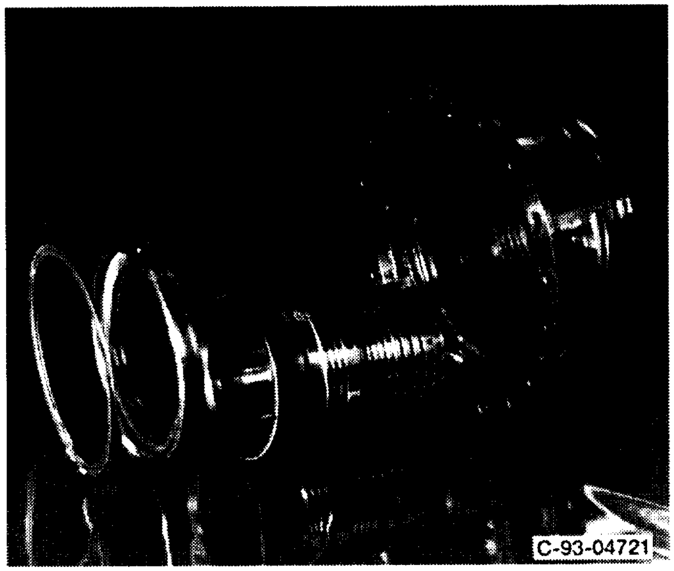

Figure 5.—Exploded view of dual-brush compressor discharge seal system (after test).

Figure 6.—Compressor discharge seal rotors for labyrinth seal (right) and brush seal (left).

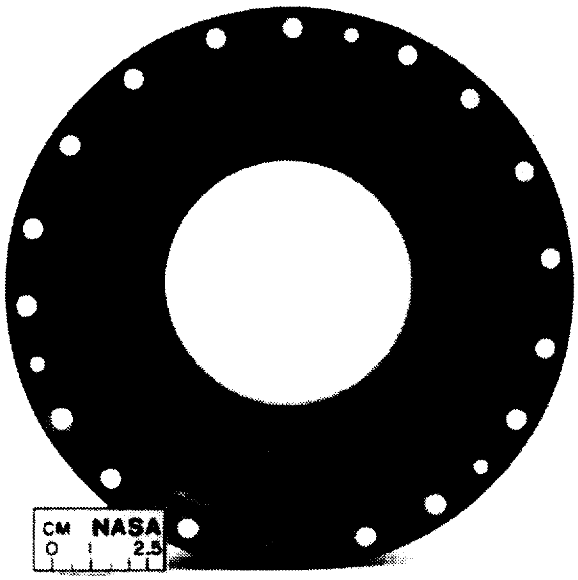

C-93-02710

(a) Upstream view.

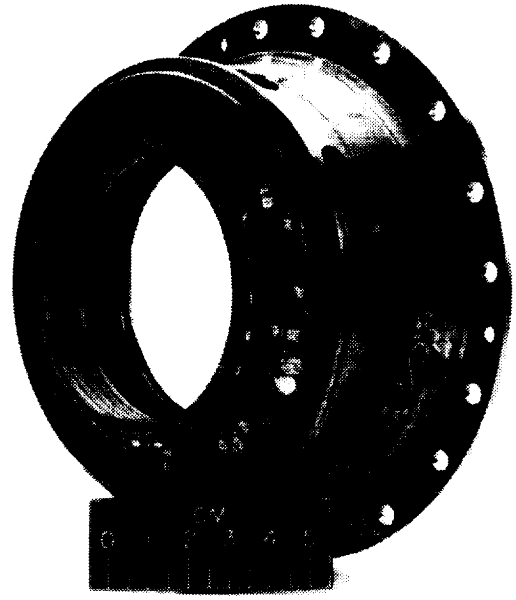

C-93-02712

(b) Downstream view.

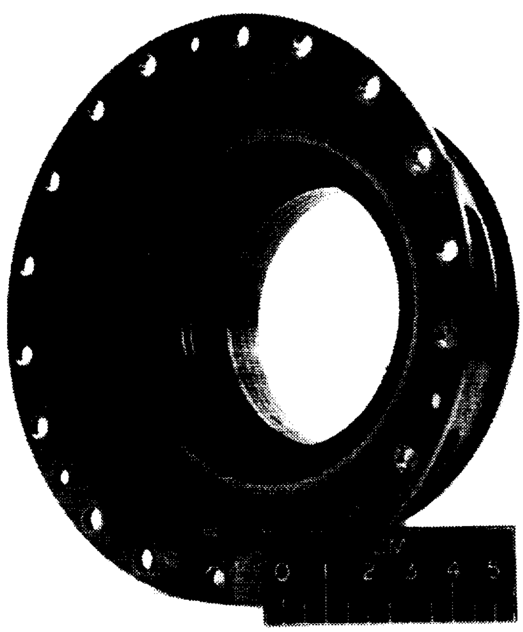

C-93-02711

(c) Isometric view.

Figure 7.—Dual-brush compressor discharge seal system after testing.

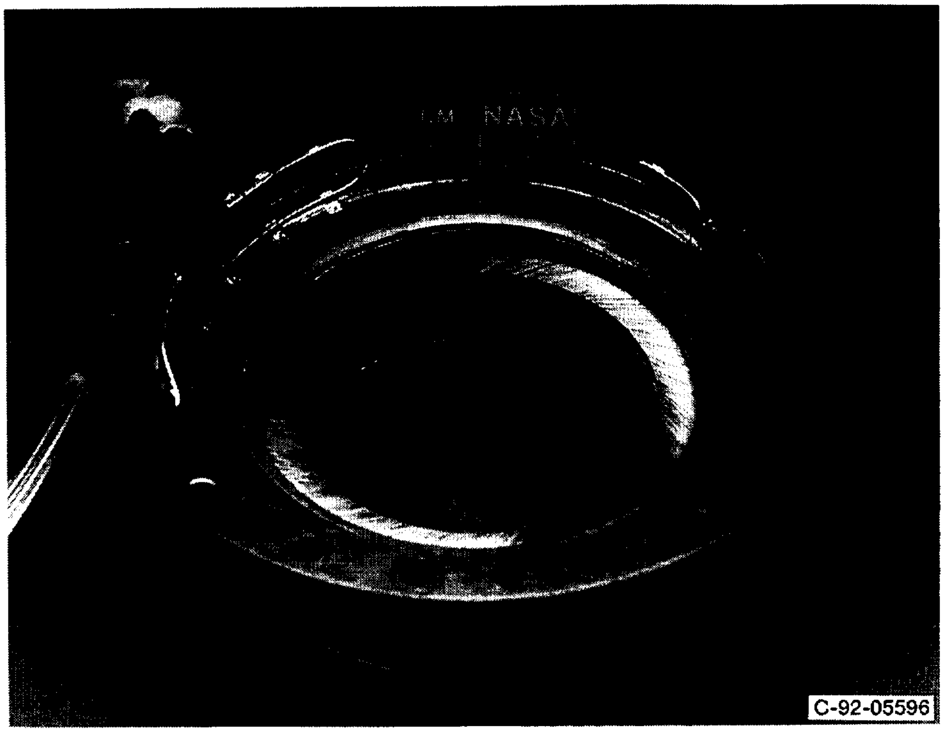

(a) Dual-brush seal.

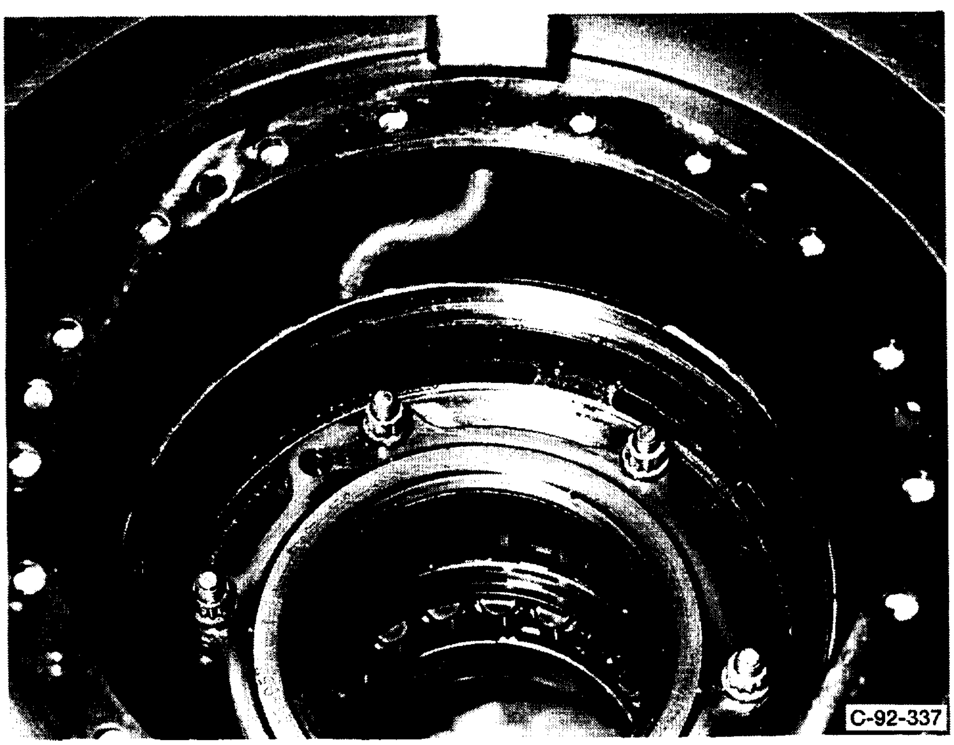

(b) Seal package cavity and housing.

Figure 8.—Dual-brush seal package installation.

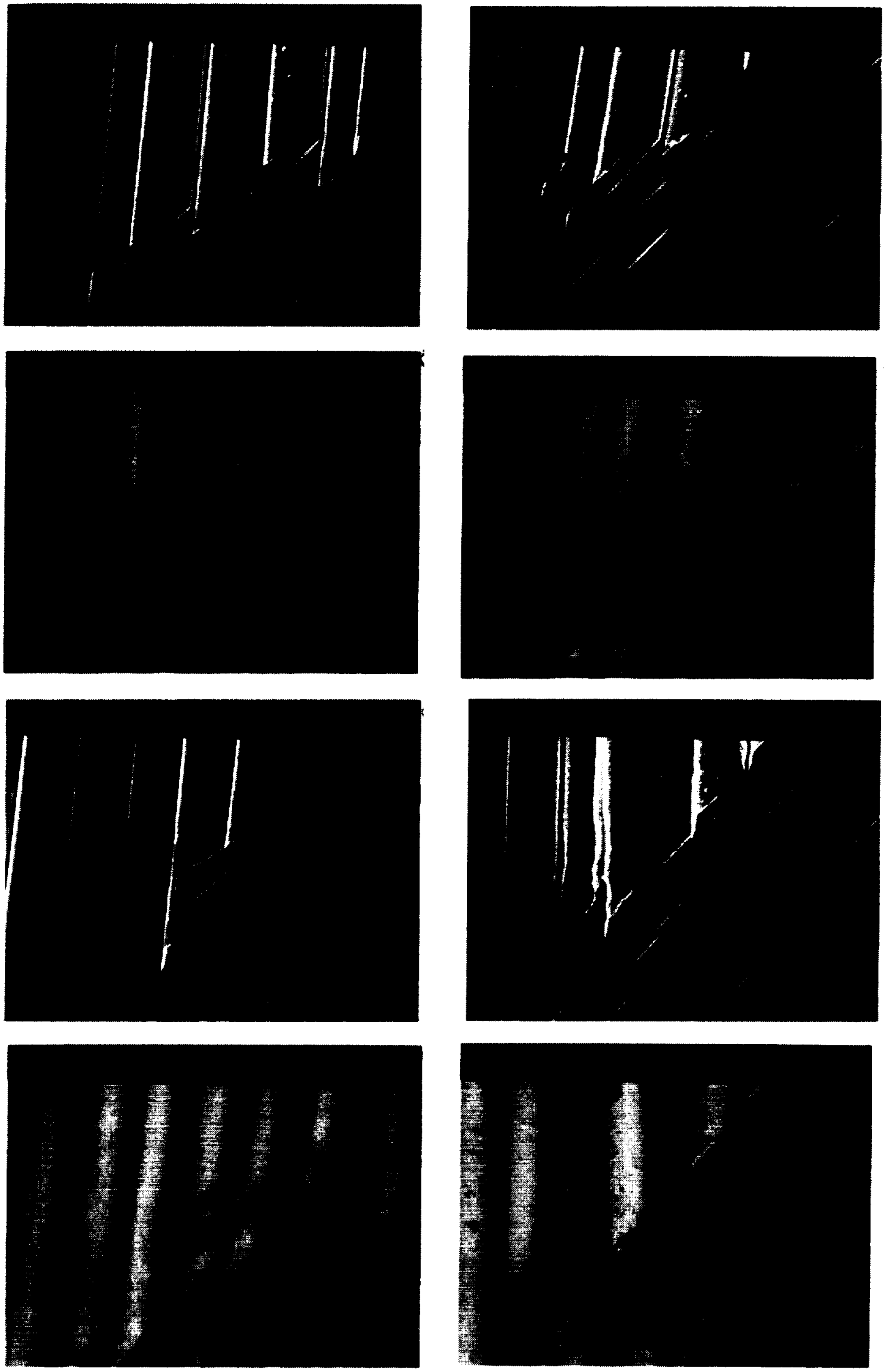

Figure 9.—Closeup views of bristles.

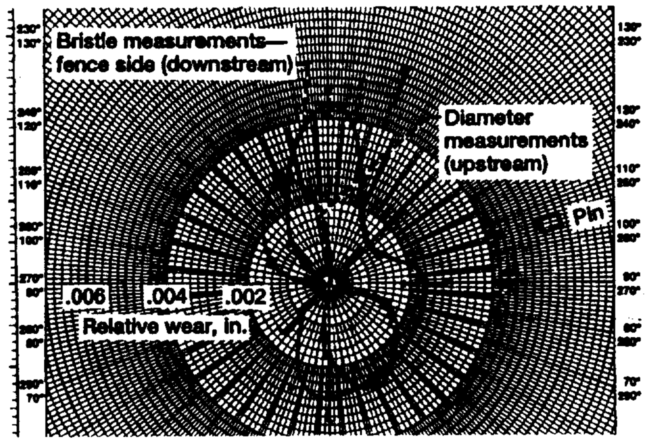

Figure 10.—Wear pattern for compressor discharge seal upstream brush.

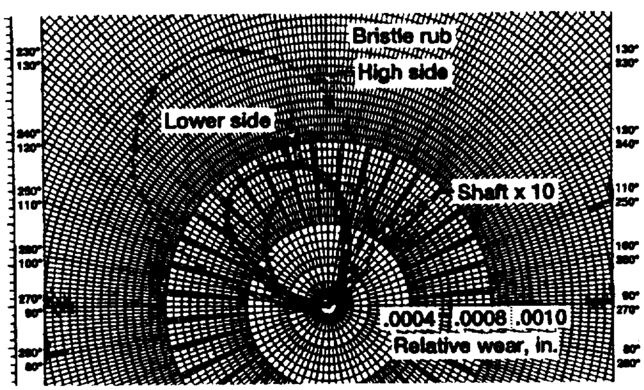

(a) Coating wear pattern.

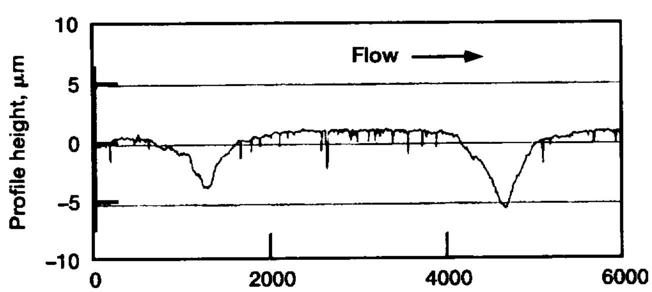

(b) Discharge seal profile showing slight wear scars.

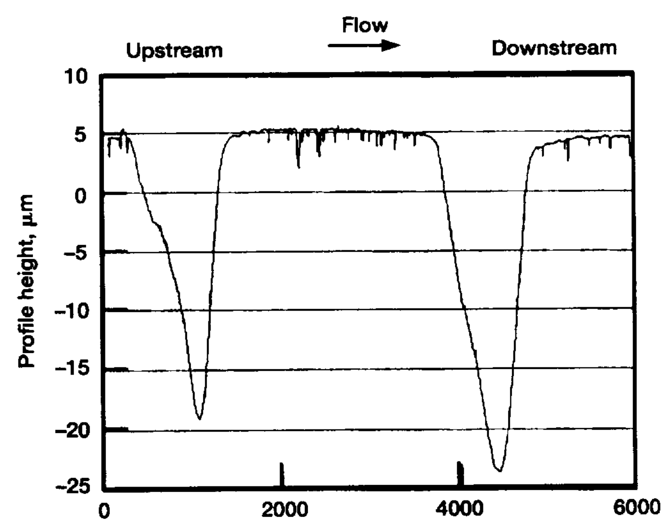

(c) Discharge seal profile showing deeper wear scars.

Figure 11.—Coating wear pattern and discharge seal profiles for compressor discharge seal rub runner.

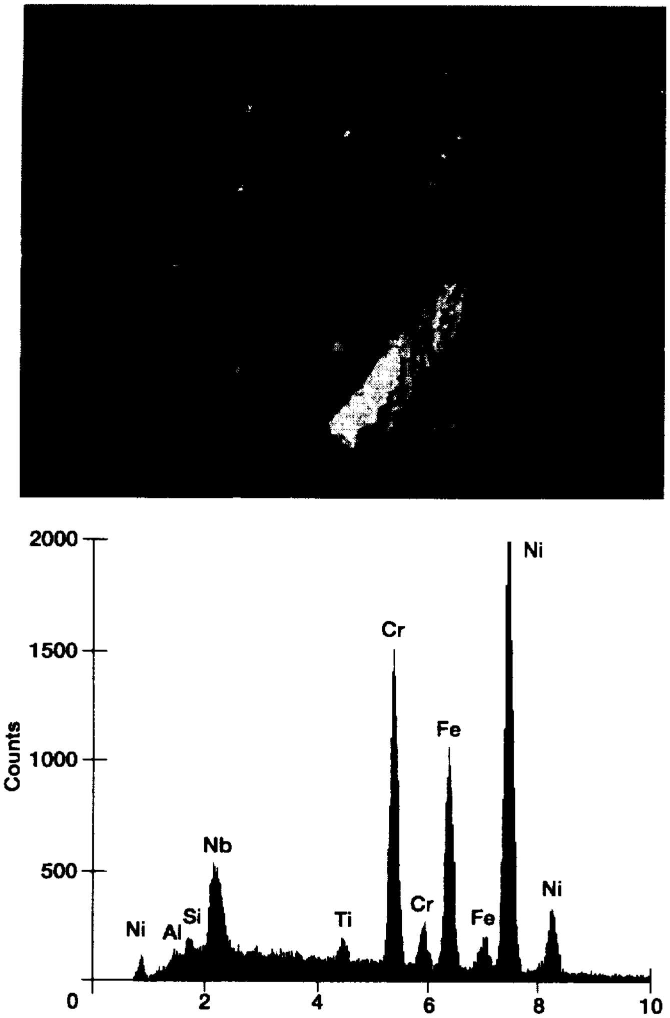

(a) Particle A.

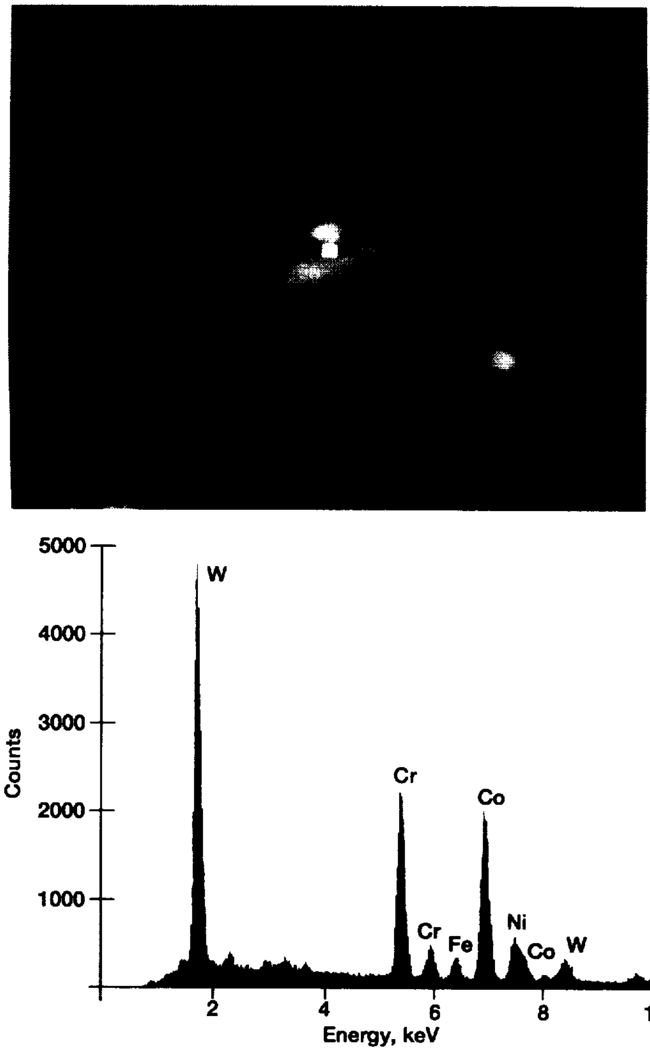

(b) Particle B.

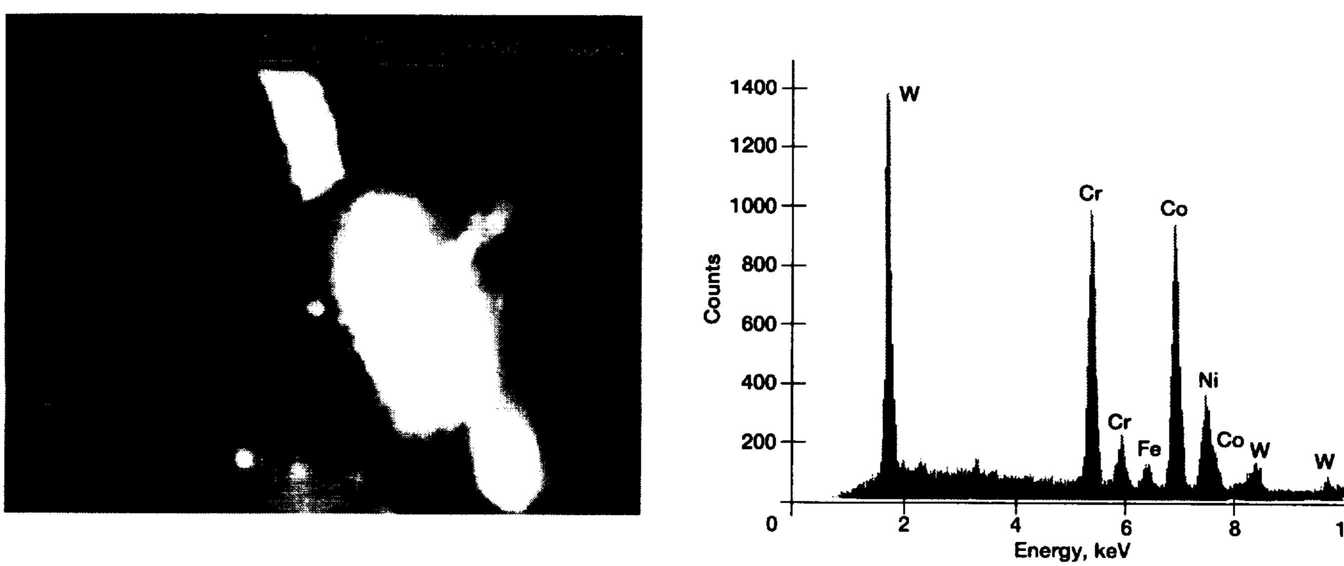

(c) Particle C.

Figure 12.—SEM peaks associated with drain pipe debris.

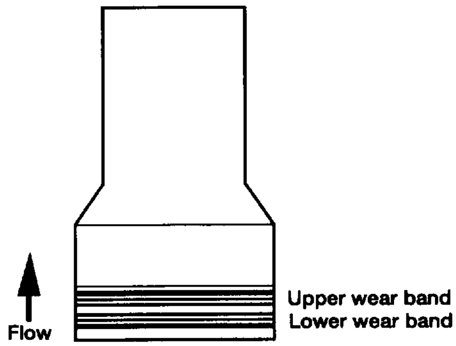

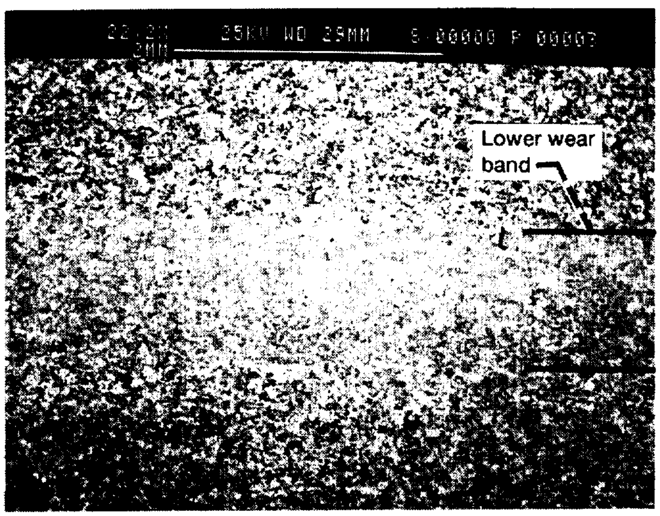

(a) Upstream (lower) wear band.

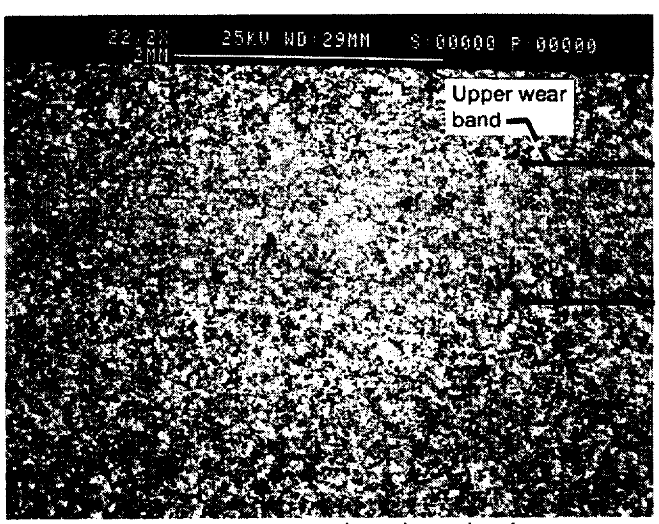

(b) Downstream (upper) wear band.

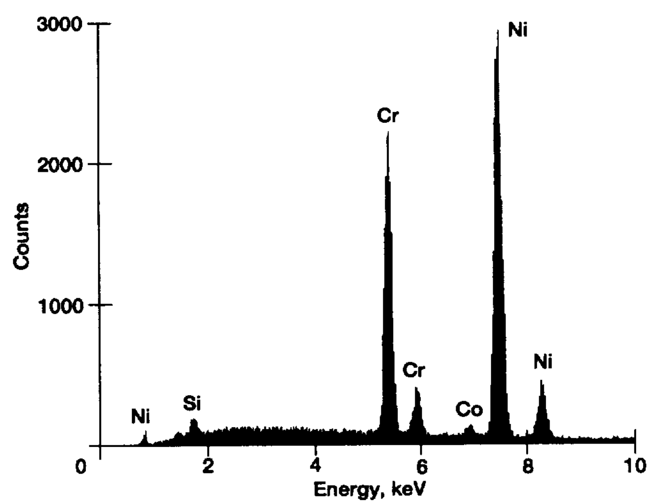

(c) Light area in coating matrix between bands.

Figure 13.—SEM peaks associated with chromium-carbide-coated rub runner.

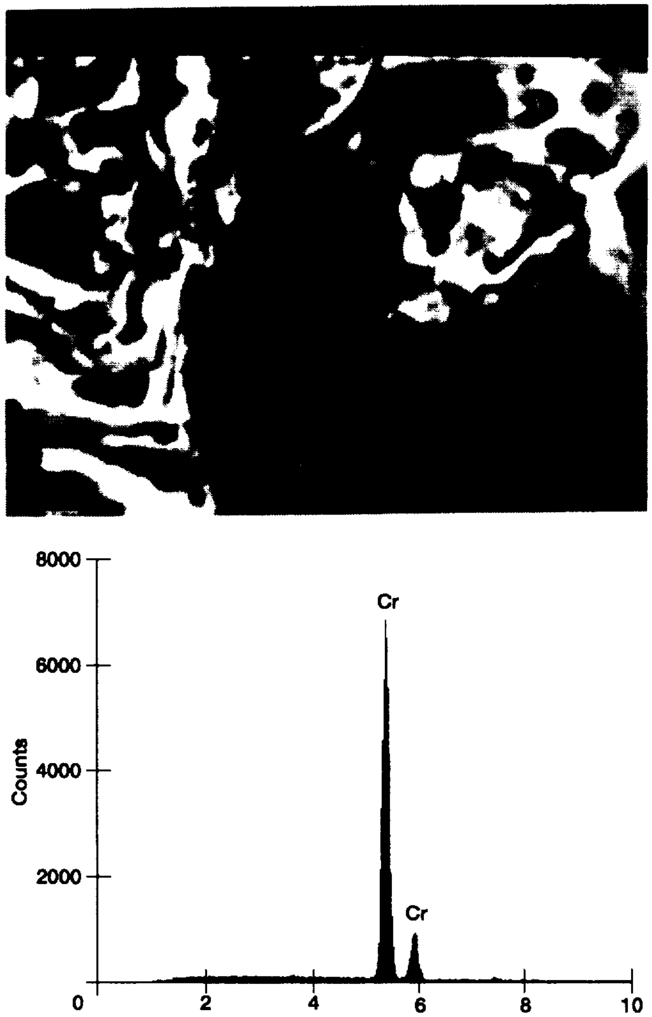

(d) Gray area in coating matrix between bands.

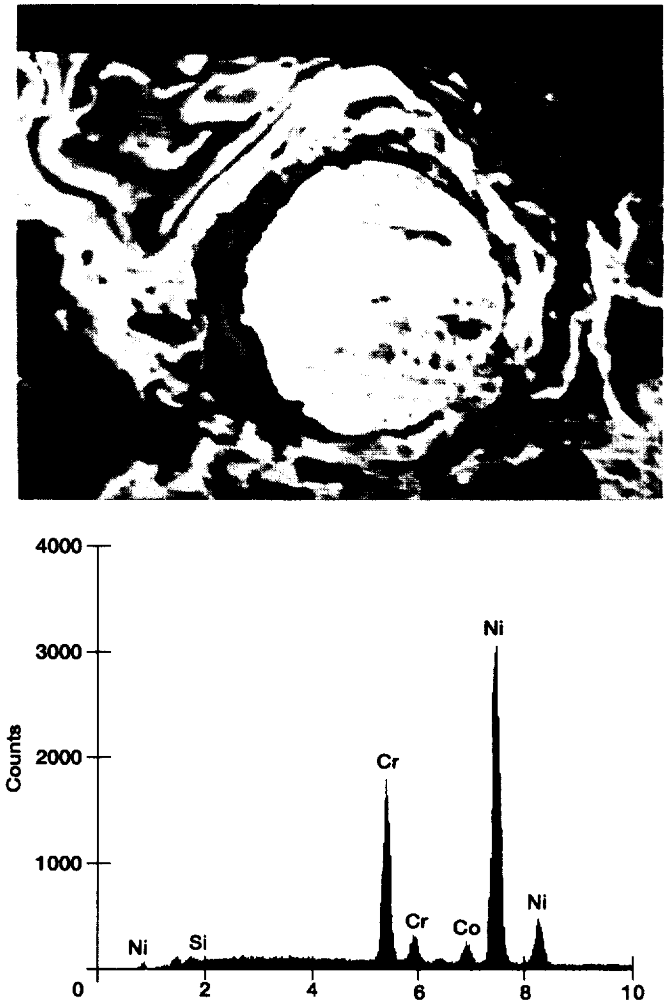

(e) Light area in upstream (lower) wear band.

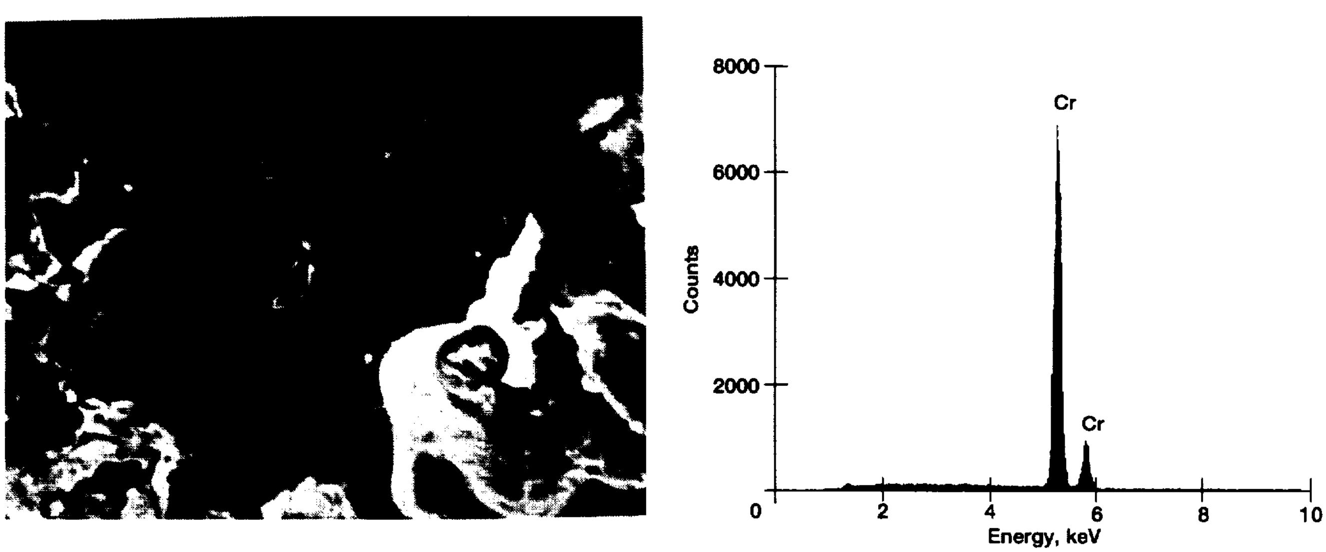

(f) Gray area in upstream (lower) wear band.

Figure 13.—Continued.

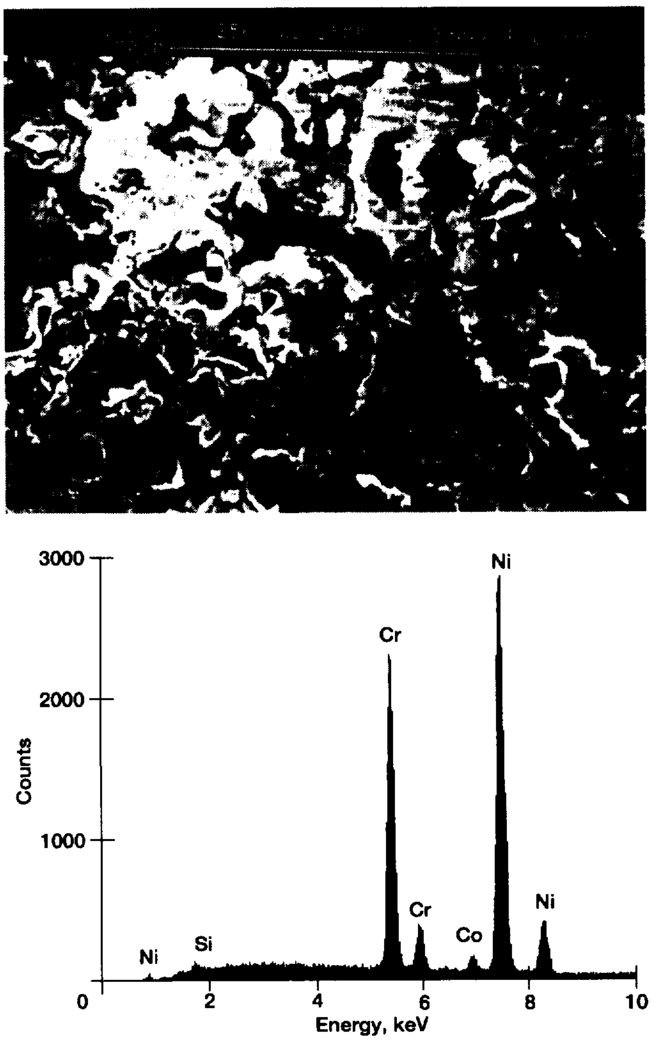

(g) Light area in downstream (upper) wear band.

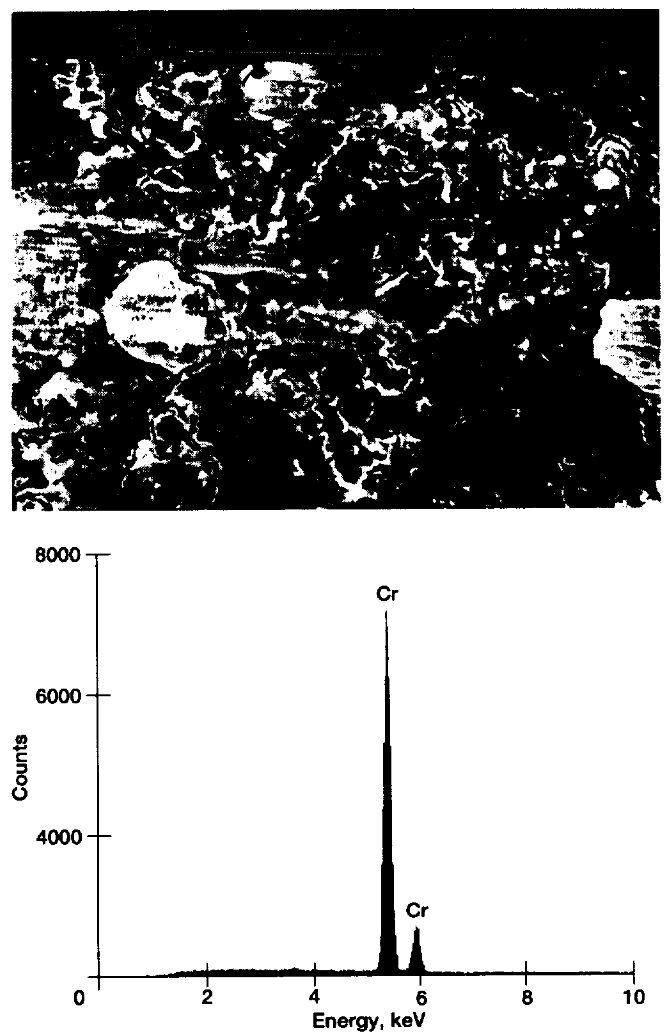

(h) Gray area in downstream (upper) wear band.

Figure 13.—Concluded.

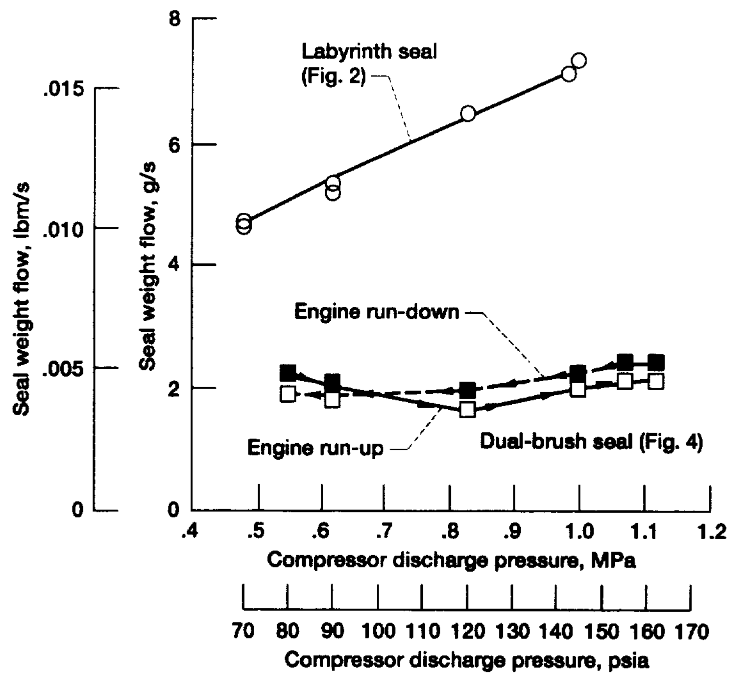

Figure 14.—Seal weight flow as a function of compressor discharge pressure for labyrinth and dual-brush seals.

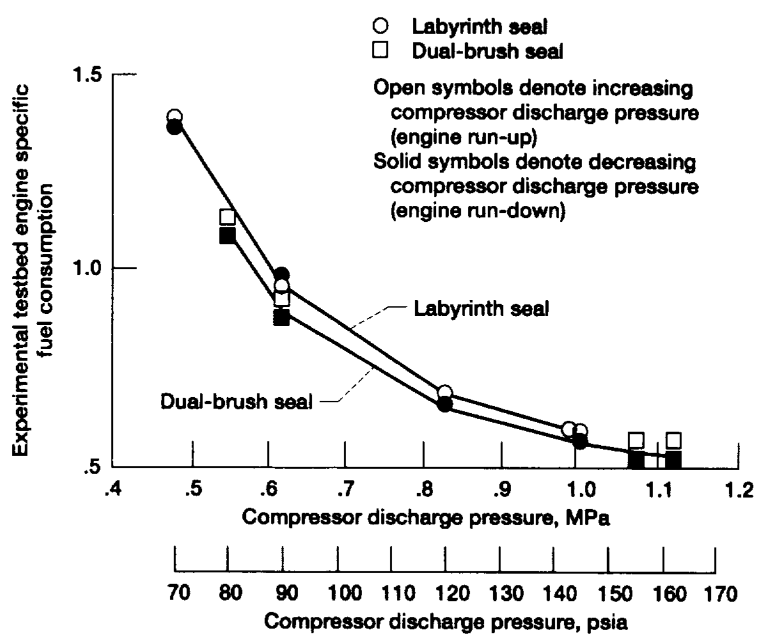

Figure 15.—Experimental testbed engine specific fuel consumption as a function of compressor discharge pressure with labyrinth and dual-brush seals.

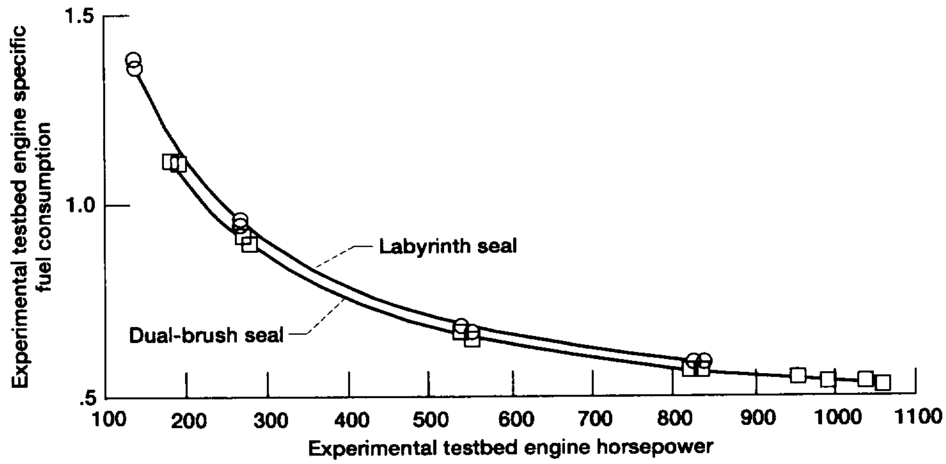

Figure 16.—Experimental testbed engine specific fuel consumption as a function of horsepower.

REPORT DOCUMENTATION PAGE

Form Approved
OMB No. 0704-0188

1. AGENCY USE ONLY (*Leave blank*)	2. REPORT DATE	3. REPORT TYPE AND DATES COVERED
	October 1995	Technical Memorandum

4. TITLE AND SUBTITLE

Relative Performance Comparison Between Baseline Labyrinth and Dual-Brush Compressor Discharge Seals in a T–700 Engine Test

5. FUNDING NUMBERS

WU–584–03–11
1L162211A47A

6. AUTHOR(S)

Robert C. Hendricks, Thomas A. Griffin, Teresa R. Kline, Kristine R. Csavina, Arvind Pancholi, and Devendra Sood

7. PERFORMING ORGANIZATION NAME(S) AND ADDRESS(ES)

NASA Lewis Research Center
Cleveland, Ohio 44135–3191
and
Vehicle Propulsion Directorate
U.S. Army Research Laboratory
Cleveland, Ohio 44135–3191

8. PERFORMING ORGANIZATION REPORT NUMBER

E–8154

9. SPONSORING/MONITORING AGENCY NAME(S) AND ADDRESS(ES)

National Aeronautics and Space Administration
Washington, D.C. 20546–0001
and
U.S. Army Research Laboratory
Adelphi, Maryland 20783–1145

10. SPONSORING/MONITORING AGENCY REPORT NUMBER

NASA TM–106360
ARL–MR–232

11. SUPPLEMENTARY NOTES

Prepared for the 39th International Gas Turbine and Aeroengine Congress and Exposition sponsored by the American Society of Mechanical Engineers, The Hague, Netherlands, June 13–16, 1994. Robert C. Hendricks, NASA Lewis Research Center; Thomas A. Griffin and Teresa R. Kline, Vehicle Propulsion Directorate, U.S. Army Research Laboratory, NASA Lewis Research Center; Kristine R. Csavina, Sverdrup Technology, Inc., Lewis Research Center Group, Brook Park, Ohio (work funded by NASA Contract NAS3–25266); Arvind Pancholi and Devendra Sood, General Electric Corporation, Lynn, Massachussets. Responsible person, Robert C. Hendricks, organization code 5300, (216) 433–7507.

12a. DISTRIBUTION/AVAILABILITY STATEMENT

Unclassified - Unlimited
Subject Category 20

This publication is available from the NASA Center for Aerospace Information, (301) 621–0390.

12b. DISTRIBUTION CODE

13. ABSTRACT *(Maximum 200 words)*

In separate series of YT–700 engine tests, direct comparisons were made between the forward-facing labyrinth and dual-brush compressor discharge seals. Compressor speeds to 43 000 rpm, surface speeds to 160 m/s (530 ft/s), pressures to 1 MPa (145 psi), and temperatures to 680 K (765 °F) characterized these tests. The wear estimate for 46 hr of engine operations was less than 0.025 mm (0.001 in.) of the Haynes 25 alloy bristles running against a chromium-carbide-coated rub runner. The pressure drops were higher for the dual-brush seal than for the forward-facing labyrinth seal and leakage was lower—with the labyrinth seal leakage being 2-1/2 times greater—implying better seal characteristics, better secondary airflow distribution, and better engine performance (3 percent at high pressure to 5 percent at lower pressure) for the brush seal. (However, as brush seals wear down (after 500 to 1000 hr of engine operation), their leakage rates will increase.) Modification of the secondary flow path requires that changes in cooling air and engine dynamics be accounted for.

14. SUBJECT TERMS

Seals; Brush; Labyrinth; Coating; Turbo shaft engine

15. NUMBER OF PAGES

23

16. PRICE CODE

A03

17. SECURITY CLASSIFICATION OF REPORT	18. SECURITY CLASSIFICATION OF THIS PAGE	19. SECURITY CLASSIFICATION OF ABSTRACT	20. LIMITATION OF ABSTRACT
Unclassified	Unclassified	Unclassified	